SIAM J. APPL. MATH.
Vol. 28, No. 4, June 1975

WAVE BREAKDOWN AND TURBULENCE*

MARTEN T. LANDAHL†

Abstract. Some new ideas on the dynamics of shear flow turbulence are presented. Central to these is the phenomenon of wave breakdown. This is defined as the onset of a violent small-scale secondary instability developing on a large-scale primary disturbance of wave-like traveling type. It is suggested that breakdown together with the ensuing violent mixing process (a turbulent "burst") constitutes the dominant nonlinear mechanism for the fluctuating velocity field in a turbulent boundary layer. A burst regeneration mechanism is proposed whereby one breakdown can excite large velocity defects in the shear flow which then may trigger a new breakdown, thus leading to self-maintenance of the turbulence.

1. Introduction. The realization that boundary layer turbulence is of a highly intermittent and "bursty" character has spurred a vigorous research in the last few years in efforts to understand the mechanism of production of turbulence near a wall. The turbulent burst phenomenon was first described by Kline and coworkers (Kline at al. (1967), Kim et al. (1971)) from visual observations of a thick, low-speed boundary layer with the aid of hydrogen bubble tracers. Their (1967) conceptual picture of a typical burst is reproduced in Fig. 1. The most important

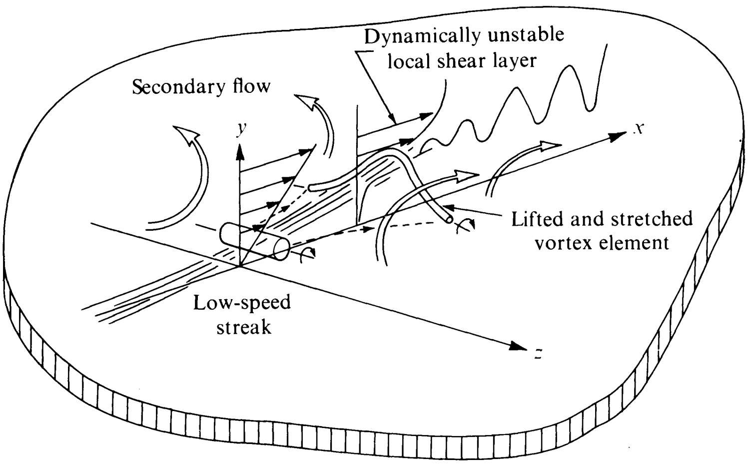

FIG. 1. *Structure of a burst.* (*From Kline, et al.*, 1967)

observation was that a burst was always initiated by a low-speed streak lifting up from the surface and forming locally a highly inflexional profile. From elementary hydrodynamic stability theory, such a profile is known to be dynamically unstable. Their suggestion that the burst is a manifestation of secondary instability induced by the large-scale fluctuations was strongly supported by the appearance of a

* Received by the editors January 30, 1974. Presented by invitation at an International Symposium on Modern Developments in Fluid Dynamics in honor of the 70th birthday of Sydney Goldstein held at Haifa, Israel, December 16–23, 1973.

† Department of Aeronautics and Astronautics, Massachusetts Institute of Technology, Cambridge, Massachusetts 02139, and The Royal Institute of Technology, Stockholm 70, Sweden. This research was supported in part by the Air Force Office of Scientific Research under Contract AF-OSR F44620-71-C-0007.

growing wave-like motion preceding the break-up of the flow. However, their later (1971) investigation showed that the oscillatory motion did not appear all of the time or even most of the time; the most prevalent flow structure just preceding break-up was a spiral, growing downstream. Corino and Brodkey (1969) further elucidated the bursting mechanism by visual studies employing a film camera moving with the flow. They found the burst to be associated with violent ejections of low-speed fluid from the wall as well as with sweeps of high-speed fluid moving towards the wall from the outer layers. Also, they identified weaker interactions between low- and high-speed regions.

For quantitative studies of the burst phenomenon, development of selective sampling techniques has become necessary, because in the usual two-point correlation measurements, the intermittency of the phenomenon will make it "drown" in the background noise. Several selective sampling schemes have been developed for this purpose. Wallace et al. (1972) classified the signal of uv according to which quadrant (determined by the signs of u, v) it belonged to. Willmarth and Lu (1973) made additional classifications depending on whether the streamwise velocity was accelerating or decelerating at the time of sampling. Also, they determined the contributions from different regions in the uv-plane by extracting the signal outside a "hole" of a given size $H = |uv|$. With this technique, events giving particularly large contributions to uv could be singled out. These measurements show that ejections of low-speed fluid from the wall and sweeps of high-speed fluids towards the wall together make up for more than 100% of the mean Reynolds stress with the balance accounted for by the wall-ward and outward interactions.

A sampling technique that especially well elucidates the nature of the bursting event is the one developed by Blackwelder and Kaplan (1972). In this, a short-time average is compared with the long-time average, and the sampling is carried out when the former exceeds the latter by some preset fraction. This scheme is heavily biased in favor of fluctuations that are completed in the sample time of the short-time average. In Figs. 2 and 3 are reproduced some of their results. Fig. 2 shows the instantaneous u-signal with the indication of the occurrence of "events" obtained from a detector probe located at $y^+ = 15$ (y^+ being the usual viscous wall variable) and with a short-time averaging (nondimensional time of $t^+ = 10$). The sample instantaneous streamwise velocity profiles, presented in Fig. 3, show a deceleration of the flow near the wall before the bursting, a distinctly inflexional profile just prior to bursting and a strong acceleration of the flow immediately thereafter, leading to an overshoot in velocity. The acceleration is followed by a comparatively slow relaxation back to the mean velocity.

It thus appears from these experiments that the bursting event is, to a certain degree, repeatable and deterministic and should therefore be amenable to a mechanistic analysis. However, no serious efforts in this direction seem as yet to have appeared in the literature.

In the present paper, an attempt is made to develop a two-scale model of the fluctuating field in a turbulent boundary layer assuming the intense turbulence arising during burst to be of much smaller scale than the turbulent fluctuations outside the bursting regions. Central to the theoretical model is also the assumption, suggested by the experimental evidence, that the nonlinear effects on the

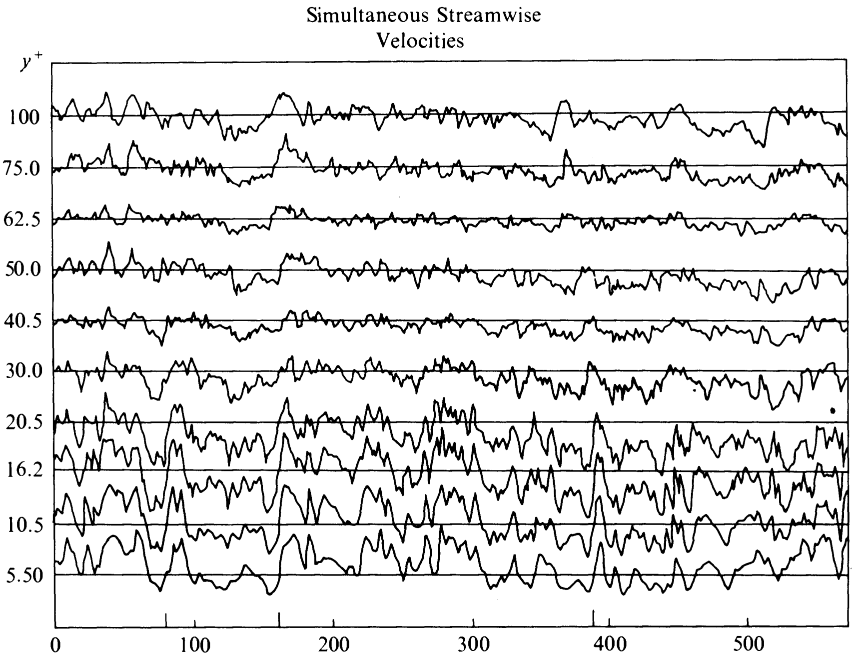

FIG. 2. *Instantaneous U-signal in the wall region of a turbulent boundary layer. (From Blackwelder and Kaplan,* 1972)

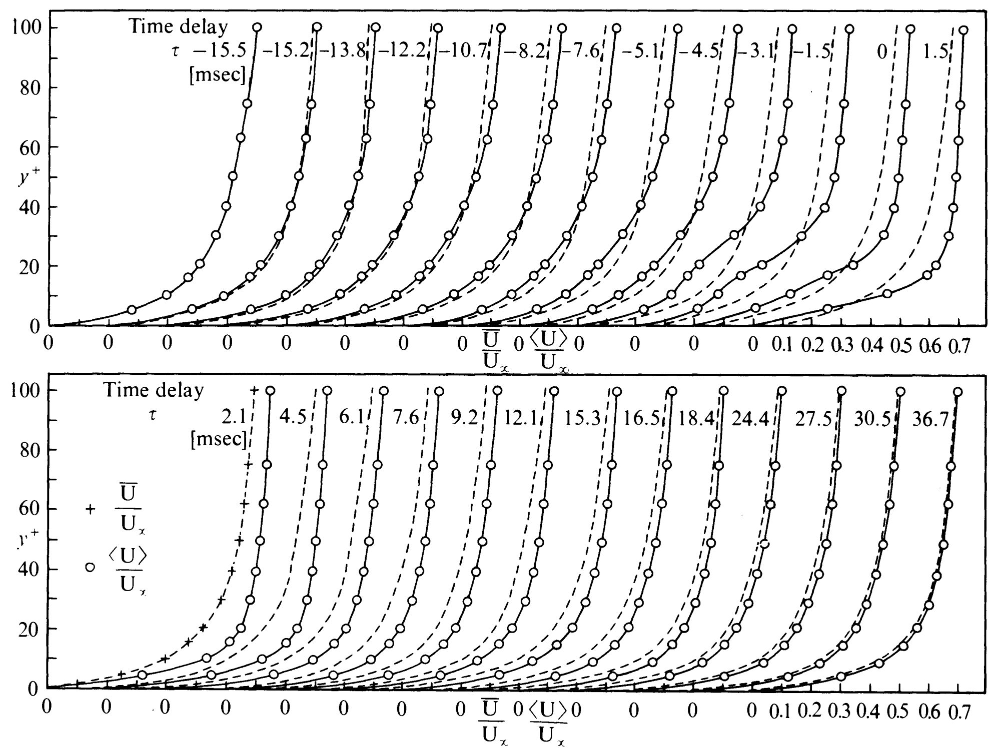

FIG. 3. *Conditionally sampled velocity profiles at various time intervals from bursts*

large-scale motion come primarily from the turbulent stresses produced by the small-scale motion. Outside the bursting regions, the flow is governed by the equation for small perturbations in a parallel flow. The strong nonlinearities are thought to arise subsequent to breakdown of the large-scale motion into secondary small-scale oscillations in the manner described by Landahl (1972b) (hereafter referred to as (I)). In this paper, it was shown how spatial nonhomogeneities could lead to focusing and trapping of small-scale secondary instabilities on traveling large-scale primary disturbances. The breakdown theory was applied to the transition problem with considerable success, and the broad similarities between turbulent spot formation and the bursting strongly suggest that both are related to the same fundamental dynamic process.

The basic conceptual model to be used here for the closure problem for the turbulent field is illustrated in Fig. 4. This model was first suggested in Landahl

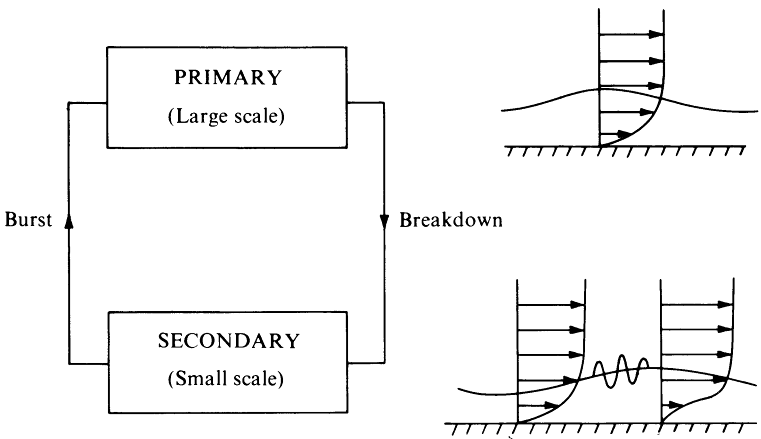

FIG. 4. *Conceptual closure model*

(1967) and further elaborated in (I) and in Landahl (1972a). A turbulent burst, initiated by a breakdown into secondary oscillations in the manner described in (I), excites the basic shear flow into large-scale fluctuations, which in turn may attain locally a critical state in the sense of the breakdown theory, giving rise to a new burst, and so on. For a turbulent shear flow to be self-sustained in this manner, there are several questions that need be answered, such as

(i) What is the strength and nature of excitation as related to the turbulent stress produced in a burst?

(ii) What is the structure of large-scale disturbances produced by a localized burst?

(iii) Can a new critical breakdown condition be caused by a single burst or must interaction between disturbances from more than one burst take place?

(iv) What is the relation of the properties of the mean velocity profile to the disturbances created by a burst?

To answer all of these questions would require the solution of the full nonlinear problem, an impossible task at present. However, some of the questions such as

(iii) and (iv) can be attacked from the basis of linear models. In the present paper, some of the tractable problems relating to the burst-primary field-structure are attacked and some tentative conclusions drawn.

2. Formulation of the two-scale model. We consider the fluctuating velocity field in a mean shear flow, which for the purpose of the present investigation shall be taken to be a parallel one. The parallel-flow assumption is exact in the case of turbulent flow in a two-dimensional channel, and should be an excellent approximation for a boundary layer in view of its slow downstream growth. Thus, setting

$$U_i = U(y)\delta_{1i} + u_i(x_j, t) \tag{1}$$

($x_1 = x,\ x_2 = y,\ x_3 = z$), where the fluctuating velocity component $u_1 = u$, $u_2 = v$, $u_3 = w$ are all assumed to have a zero mean, we obtain after substitution into the Navier–Stokes equations and subtraction of the mean field the following set of equations:

$$\frac{\partial u_i}{\partial t} + U\frac{\partial u_i}{\partial x} + v\frac{dU}{dy}\delta_{1i} = -\frac{1}{\rho}\frac{\partial p}{\partial x_i} + \nu\nabla^2 u_i + \frac{\partial \tau_{ij}}{\partial x_j}, \tag{2}$$

$$\frac{\partial u_i}{\partial x_i} = 0, \tag{3}$$

where the fluctuation turbulent stress terms τ_{ij} are given by

$$\tau_{ij} = \overline{u_i u_j} - u_i u_j. \tag{4}$$

By elimination of the pressure from (2), one obtains with the aid of (3) the following equation for the velocity component $u_2 = v$ (Landahl (1967)):

$$\left(\frac{\partial}{\partial t} + U\frac{\partial}{\partial x}\right)\nabla^2 v - U'' v_x - \nu\nabla^4 v = q, \tag{5}$$

where

$$\begin{aligned} q &= \frac{\partial}{\partial x_j}\left(\frac{\partial^2 \tau_{ij}}{\partial x_i \partial x_2} - \frac{\partial^2 \tau_{2j}}{\partial x_k \partial x_k}\right) \\ &\equiv \left(2\frac{\partial^2}{\partial y^2} - \nabla^2\right)[(uv)_x + (vw)_z] \\ &\quad + [(u^2 - v^2)_{xx} + (w^2 - v^2)_{zz} + 2(uw)_{xz}]_y. \end{aligned} \tag{6}$$

Since the right-hand side of (5) involves quadratic terms containing all the velocity components u_i, it is useful as a model equation only if either

(a) the perturbations are small so that the nonlinear terms may be neglected everywhere, or,
(b) the nonlinear terms are weak and can be found by iteration, or,
(c) the nonlinear terms are strong only in localized regions in time and space so that they give rise to "compact" sources q.

The case (a) is the one considered in hydrodynamic stability theory, and a Fourier transform of the linear left-hand side of (5) gives the usual Orr–Sommerfeld equation to be further discussed below. Case (b) is the one usually assumed in nonlinear hydrodynamic stability theories of the Landau–Stuart variety.

In a turbulent boundary layer, all small disturbances appear to be damped (Landahl (1967)) so that nonlinearities must be important, at least in some regions of space and time, in order to maintain the turbulence. The experiments such as those cited above strongly suggest that the turbulent velocity field consists mainly of patches of intense small-scale turbulence of an intermittent and "bursty" nature separated by regions of laminar-like but unsteady motion of larger scale.

We shall therefore, in the model to be developed, assume that the turbulent field consists of a superposition of two scales of motion, a larger-scale one of characteristic scale $\tilde{\lambda}$ being typically of order of, say, the boundary layer displacement thickness, and a smaller-scale one of characteristic scale λ' being typical of the thickness of the viscous wall layer (see Fig. 5). The patches of intense small-scale

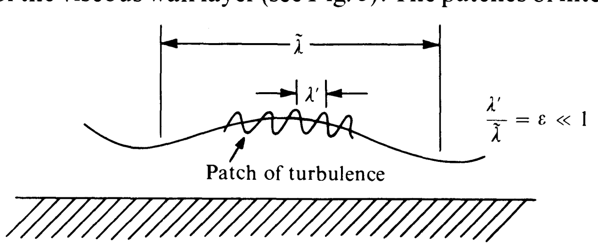

FIG. 5. *Two-scale model of turbulent field*

turbulence would have streamwise and spanwise dimensions of order $\tilde{\lambda}$ or smaller but which are much greater than λ'. The patches are considered to arise from breakdown into secondary instability of the large-scale motion, and their y-extent would therefore be of order λ'. For a formal decomposition of the field into large- and small-scale component, we set, accordingly,

$$u_i = \tilde{u}_i + u_i', \tag{7}$$

where $\tilde{u}_i$ represents the large-scale and u_i' the small-scale motion with characteristic scales $\tilde{\lambda}$ and λ', respectively. The large-scale velocity field $\tilde{u}$ would be the one detected with selective sampling techniques such as the one used by Blackwelder and Kaplan (1972). Equations of motion for the large- and small-scale fields are obtained by substituting (7) into (6), taking the selective sampling average to produce an equation for $\tilde{u}_1$. This is then subtracted from (6) to find the equation for u_i'. Next, these are simplified by neglecting terms that are of higher order in the small quantity

$$\varepsilon = \lambda'/\tilde{\lambda}. \tag{8}$$

This procedure leads to an equation for $\tilde{v}$ which may schematically be written as follows:

$$\begin{aligned}\left(\frac{\partial}{\partial t} + U\frac{\partial}{\partial x}\right)\nabla^2\tilde{v} - U''\tilde{v}_x - \nu\nabla^4\tilde{v} &= [(\widetilde{u'v'})_x + (\widetilde{v'w'})_z]_{yy} \\ &\quad + \text{(higher order terms in } \varepsilon).\end{aligned} \tag{9}$$

Terms involving higher order x- and z-derivatives are neglected compared to those involving y-derivatives, since the latter will be set by the small scale (see Fig. 5), while the former will be determined by the x- and z-dimensions of the patch of small-scale turbulence, which were assumed to be several times the small scale. Possibly, the most questionable assumption in (9) lies in neglecting truly nonlinear terms such as

$$(\tilde{u}\tilde{v})_{xyy}$$

compared to the ones retained involving the small-scale components u_i', only. To justify this, one would have to check afterwards from the solution obtained whether such terms are indeed small.

The equation for the small-scale component v' reads

$$\left(\frac{\partial}{\partial t} + \tilde{U}\frac{\partial}{\partial x} + \tilde{w}\frac{\partial}{\partial z}\right)\nabla^2 v' - \tilde{U}_{yy}v_x' - \tilde{w}_{yy}v_z' - \nu\nabla^2 v' = q' + (\text{linear terms of higher order in } \varepsilon), \tag{10}$$

where q' stands for the nonlinear source terms obtained by replacing u_i by u_i' in (6) and $\tilde{U} = U + \tilde{u}$. The linear terms stated to be of higher order involve higher order x- and z-derivatives of the large-scale field $\tilde{u}_i$.

The equations of motion for the individual velocity components may be treated in an analogous manner as needed, but we will postpone writing them down until later.

3. The small-scale field. In the two-scale model, the nonlinearities of the problem only appear directly in the equation for the small-scale field. The equation for $\tilde{v}$, on the other hand, only contains the nonlinearity indirectly through the effect of the large-scale field on the Reynolds stress terms $\widetilde{u'v'}$ and $\widetilde{v'w'}$. A complete analysis of the small-scale motion is therefore exceedingly difficult, and one would have to confine oneself to the initial phase of the small-scale motion, which is initiated by secondary instability and breakdown. Since the instability is of inflexional type, viscosity may be neglected, and omitting nonlinear terms in (10) as well, one obtains

$$\left(\frac{\partial}{\partial t} + \tilde{U}\frac{\partial}{\partial x} + \tilde{w}\frac{\partial}{\partial z}\right)\nabla^2 v' - \tilde{U}_{yy}v_x' + \tilde{w}_{yy}v_z' = 0. \tag{11}$$

With the aid of a simple rotation of the coordinate system in the spirit of Squire's transformation, this may be written

$$\left(\frac{\partial}{\partial t} + \tilde{U}_*\frac{\partial}{\partial x_*}\right)\nabla_*^2 v' - \tilde{U}_{*yy}v_{x*}' = 0, \tag{12}$$

where starred variables refer to a coordinate system with the x_*-axis aligned locally with the large-scale flow. We thus have the Rayleigh stability problem for the large-scale flow, which tells that instability arises whenever the mean shear $\partial\tilde{U}_*/\partial y$ has a maximum in the interval. In assessing when the instability is likely to become explosive, one has to take into account that the field $\tilde{u}_i$ is slowly varying in time and space as seen in the scale of u_i'. This problem was addressed in (I), in which it was shown that a critical condition for breakdown into strong secondary instability is reached when, for a two-dimensional instability wave, its group velocity, calculated on the basis of the local instantaneous velocity profile, becomes equal to the phase velocity, c_0, of the large-scale traveling inhomogeneity. For a large-scale inhomogeneity not of a traveling-wave type, the equivalent phase velocity, c_0, could be determined from the temporal and spatial variations of the group velocity, c_g', for the secondary instability from the expression

$$c_0 = -(c_g')_t/(c_g')_x, \tag{13}$$

where the partial derivatives are to be determined holding the wave number constant. In (I) it was also shown how the breakdown criterion could be extended to three-dimensional waves by considering the group and phase velocity components normal to an oblique primary wave front. In (I), only the two-dimensional problem was treated in detail. In a fully three-dimensional situation, the search for the appearance of a critical state becomes quite cumbersome since it would involve, for each large-scale disturbance field considered, a calculation of c_g' for a range of wave numbers at all x, z, t-points in the flow so that the equivalent c_0 and sweep angle of the traveling disturbance can be calculated. From the observations by Kim et al. (1971), which showed that the bursting was preceded in a majority of cases by a growing spiral disturbance, one would tentatively conclude that the secondary disturbance is a highly swept one so that oblique wave breakdowns would probably be the dominating feature (see Fig. 7). This

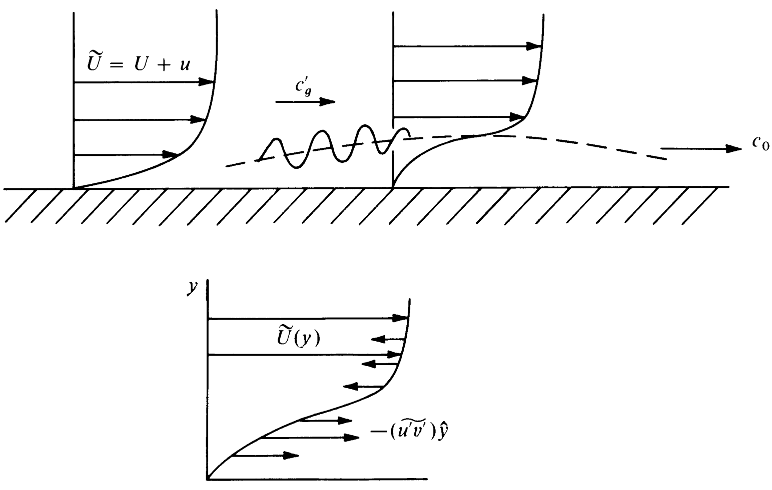

FIG. 6. *Small-scale field*

possibility is also supported by the present model which shows (see below) that the large-scale $\tilde{u}$-disturbances produced by a localized burst tends to elongate in the streamwise direction. Whether the breakdown is straight or oblique would have important consequences for the relative contributions of the stresses $\widetilde{u'v'}$ and $\widetilde{v'w'}$ to the source term for the large-scale motion.

Consider the case of an unswept breakdown. A wave-like disturbance of the form

$$v' = -i\alpha'\psi(y, z)\, e^{i\alpha'(x - c't)},$$

where ψ varies only slowly with z, is to be found from the solution of

$$(\tilde{U} - c')(\psi_{yy} - \alpha'^2\psi) - \tilde{U}_{yy}\psi = 0. \tag{14}$$

The Reynolds stress $\widetilde{u'v'}$ given by such a disturbance can be shown to be given by (Lin, 1955, p. 54)

$$(\widetilde{u'v'})_y = -\frac{c_i'\tilde{U}_{yy}}{2\alpha'|\tilde{U} - c'|^2}|\tilde{v}'|^2. \tag{15}$$

For inflexional instability with $c_i' > 0$, the stress will thus be such as to tend to retard the flow above the inflexion point and speed it up below it, i.e., to tend to smooth out the inflexional region and hence stabilize the secondary disturbance (Fig. 6). This will therefore only continue to grow for a short time before the local

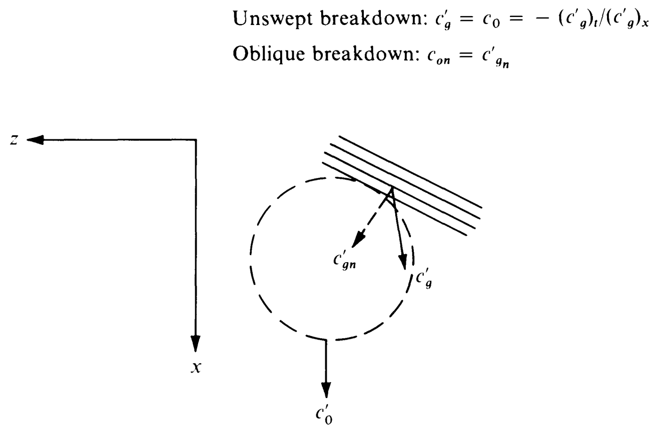

FIG. 7. *Oblique breakdown*

velocity profile has become stabilized. At this stage, the Reynolds stress will vanish. The amplitude of v' is set both by its growth due to the instability and by space-time focusing in the manner discussed in (I). The breakdown criterion

$$c_g' = c_0 \tag{16}$$

also ensures that the secondary wave packet will travel along with the primary inhomogeneity to allow amplitudes to build up. The picture that emerges is thus one of rapid build-up of the Reynolds stress $\widetilde{u'v'}$ which, as can be concluded from (1), will be negative, but which will rapidly decay to zero when the local inflexion region has been smoothed out. Therefore, on the time scale of $\tilde{u}_i$, $\widetilde{u'v'}$ may have the appearance of a short (negative) pulse. The strength and duration of the pulse cannot be determined without consideration of the full nonlinear problem.

For the straight breakdown, the velocity component w' would arise from variations of the amplitude of v' in the spanwise direction, and will thus be of order $\varepsilon u'$. Hence, $\widetilde{v'w'} = O(\varepsilon u'v')$ and can therefore be neglected. For oblique breakdowns, however, u' and w' may be of the same order and both terms must be retained. As will be shown below, the stress component $\widetilde{v'w}$ is likely to be the most essential one for the initiation of disturbances leading to a new burst.

4. The large-scale field. We will now consider the short- and long-time behavior of the large-scale field. The short-time behavior can be found from the component equations (2) under the assumption that convective and viscous terms and pressure gradients in the x- and z-directions are all negligible compared to the turbulent stresses produced during the burst. The correctness of this assumption is readily established as far as the convective and viscous terms are concerned, but the neglect of the pressure gradient requires a check a posteriori. By this assumption, the first and third of (2) may be approximated as

(17) $$\tilde{u} \simeq (\widetilde{u'v'} - \overline{uv})_y,$$

(18) $$\tilde{w}_t \simeq -(\widetilde{v'w'})_y,$$

which, upon neglecting the mean shear stress in (17) compared to the high instantaneous value arising during the burst, give

(19) $$\tilde{u} - \tilde{u}_0 \simeq -\tilde{f}_{1y},$$

(20) $$\tilde{w} - \tilde{w}_0 \simeq -\tilde{f}_{3y},$$

where

(21) $$\tilde{f}_1 = \int_0^t \widetilde{u'v'}\, dt,$$

(22) $$\tilde{f}_3 = \int_0^t \widetilde{v'w'}\, dt,$$

and where index 0 denotes initial values. From the continuity equation, $\tilde{v}$ is found to be

(23) $$\tilde{v} - \tilde{v}_0 = \tilde{f}_{1x} + \tilde{f}_{3z}.$$

The pressure may now be determined by integration of the second of the component equations, which gives

(24) $$\tilde{p} - \tilde{p}_0 = \rho\left\{\int_y^\infty 2\,[(\widetilde{u'v'})_x + (\widetilde{v'w'})_z]\, dy - \widetilde{v'^2}\right\},$$

from which the justification for neglecting the pressure gradient terms in the equations for $\tilde{u}$ and $\tilde{w}$ can be shown to follow.

At this stage, it is appropriate to discuss the effects of viscosity, which was neglected in the above approximate solutions. In the very first instants before the Reynolds stresses created by the burst have had time to induce any substantial change in the large-scale flow, the acceleration of the fluid particles would be given solely by the additional turbulent stress terms, the initial flow being driven by its own associated pressure gradients and viscous stresses. The total changes in $\tilde{u}$ and $\tilde{v}$ during the bursting will be of the same order as those of the initial distributions $\tilde{u}_0$ and $\tilde{v}_0$, themselves, so that the additional viscous stresses present after the rapid change in $\tilde{u}$ and $\tilde{v}$ has been completed will be of the same order as those of the initial velocity field. Hence, the additional viscous stresses, when fully developed, will give rise to accelerations typical of the large-scale field during off-bursting periods, which are much smaller than those typical of the bursting phase. Thus, one would conclude that the viscous stresses could be neglected altogether.

The short-time effect of a turbulent burst can be more clearly understood by taking the moment of the velocity changes. Using the short-time approximations for $\Delta\tilde{v} = \tilde{v} - \tilde{v}_0$, etc., and performing integrations by parts assuming $\tilde{f}_1$ and $\tilde{f}_3$ to vanish at the wall and outside the turbulent patch, one obtains

$$\iiint y\Delta\tilde{u}\, dV = \iiint \tilde{f}_1\, dV < 0, \tag{25}$$

$$\iiint x\Delta\tilde{v}\, dV = -\iiint \tilde{f}_1\, dV > 0, \tag{26}$$

$$\iiint z\Delta\tilde{v}\, dV = -\iiint \tilde{f}_3\, dV, \tag{27}$$

$$\iiint y\Delta\tilde{w}\, dV = \iiint \tilde{f}_3\, dV. \tag{28}$$

Furthermore,

$$\iiint \Delta\tilde{u}_i\, dV = 0, \tag{29}$$

i.e., the linear momentum is redistributed during the burst in such a way as to add an (almost) impulsive moment of momentum to the large-scale flow with components

$$\tilde{M}_{(x)} = -2\rho \iiint \tilde{f}_3\, dV, \tag{30}$$

$$\tilde{M}_{(z)} = -2\rho \iiint \tilde{f}_1\, dV. \tag{31}$$

For an unswept breakdown, the moment vector will have a z-component only, with a sign (for negative $\tilde{f}_1$) such as to accelerate the fluid towards the wall in the region upstream of the burst and away from the wall in the region downstream. For a swept breakdown, one would expect the moment vector to be approximately aligned with the front of the small-scale wave producing breakdown. The kinetic energy for the burst is supplied through the redistribution of the velocity so as to cancel out the internal shear layer.

The picture that emerges for the short-time behavior of the large-scale velocity field induced by an unswept burst can be illustrated qualitatively as shown in Fig. 8. In the upstream regions of the burst where $\partial\tilde{f}_1/\partial x$ is negative,

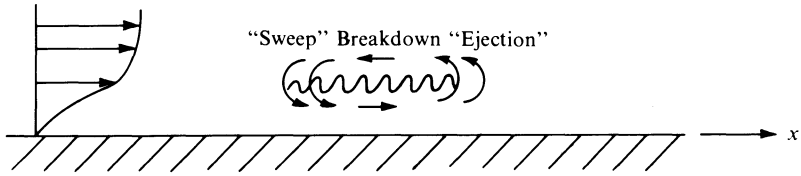

FIG. 8. *Flow structure in burst*

there will be an acceleration of the flow towards the wall, and in the downstream regions the acceleration will be away from the wall. Near the wall, there will be a rapid acceleration in the streamwise direction, and a less intense deceleration at larger distances from the wall. The picture is highly suggestive of the ejection and sweep stages described by Corino and Brodkey (1969), and by the rapid streamwise acceleration seen in the experiments of Blackwelder and Kaplan (1972). The latter do not show any evidence of deceleration in the regions away from the wall, however.

Before proceeding to study the long-time behavior of the large-scale field in detail, we will consider what will happen to the $\tilde{u}$-field if the bursts were turned off altogether at time $t = 0$. Then

$$\tilde{u}_t = (\overline{uv})_y + \nu\tilde{u}_{yy}\,, \tag{32}$$

and thus for moderate times before viscosity becomes important,

$$\tilde{u} - \tilde{u}_0 = t(\overline{uv})_y \simeq \mu t U'', \tag{33}$$

where we have used the approximation that $\overline{uv} + \mu U' \simeq$ const. in the constant-stress region. Thus, in the absence of stress-producing bursts, the flow would slow down, the deceleration being largest in the range $5 < y^+ < 50$ in which the mean profile curvature has its largest negative values. The fluctuating velocities near the wall would therefore have a tendency to a slow drift towards negative values between bursts, as illustrated conceptually in Fig. 9. The bursts must therefore be

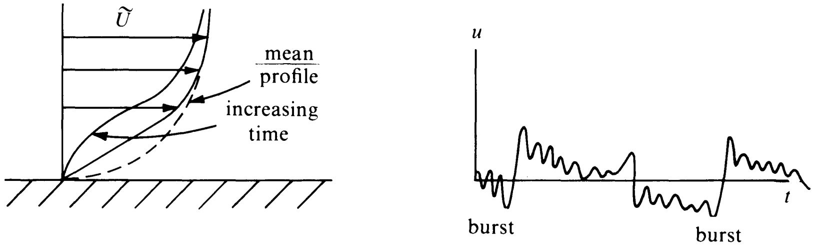

FIG. 9. *Typical behaviour of the fluctuating field between bursts*

sufficiently strong to make the u-velocity overshoot the mean in order that the mean of u be zero. On examining the data from Blackwelder and Kaplan (1972) (see Fig. 2), one sees indeed evidence of such a tendency.

In the remainder, we will ignore the effect of the mean stress in analyzing the large-time behavior of $\tilde{u}$. To determine the $\tilde{v}$-field induced by a burst in the time period immediately following it, we need to solve the homogeneous problem

$$\left(\frac{\partial}{\partial t} + U\frac{\partial}{\partial x}\right)\nabla^2\tilde{v} - U''\tilde{v}_x - \nu\nabla^4\tilde{v} = 0 \tag{34}$$

with initial conditions specified by the solution (23), viz.,

$$\tilde{v}_{t=t_1} \equiv \tilde{v}_1 = \tilde{v}_0 + (\tilde{f}_{1x} + \tilde{f}_{3z})_{t=t_1}, \tag{35}$$

time $t = t_1$ referring to the time of completion of the small-scale bursting. For $t > t_1$, the model adopted thus assumes that insignificant turbulent stresses are produced, and that all nonhomogeneous terms in (5) may consequently be ignored. The initial value problem thus posed with homogeneous boundary conditions at $y - 0$ and $y = \infty$ is readily attacked with the aid of an eigenfunction procedure in the standard manner (see, e.g., Eckhaus (1965)). First, we apply a Fourier transform in x and z by setting

$$\hat{v}(y, t; \mathbf{k}) = \iint_{-\infty}^{\infty} \tilde{v}\, e^{-i\mathbf{k}\cdot\mathbf{r}}\, d\mathbf{r}, \tag{36}$$

where

$$\mathbf{k} = (\alpha, \beta), \qquad \mathbf{r} = (x, z).$$

This gives, with suitable nondimensionalization, the following problem:

$$\left(\frac{\partial}{\partial t} + i\alpha U\right)(D^2 - k^2)\hat{v} - i\alpha U''\hat{v} - R^{-1}(D^2 - k^2)^2\hat{v} = 0, \tag{37}$$

$$\hat{v}(y, t_1; \mathbf{k}) \equiv \hat{v}_1 = \iint_{-\infty}^{\infty} \tilde{v}_1\, e^{-i\mathbf{k}\cdot\mathbf{r}}\, d\mathbf{r}, \tag{38}$$

where $D = \partial/\partial y$, $R =$ Reynolds number, with the boundary conditions that $\hat{v} = 0$ and $D\hat{v} = 0$ for $y = 0$ and $y = \infty$. The solution of this initial value problem reads

$$\hat{v} = \sum_{n=0}^{\infty} \hat{A}^{(n)}\phi^{(n)}(y)\, e^{-i\alpha c^{(n)}t}, \tag{39}$$

where $\phi^{(n)}$ and $c^{(n)}$ are the eigensolutions and eigenvalues, respectively, of the Orr–Sommerfeld equation

$$(U - c)(D^2 - k^2)\phi - U''\phi - \frac{1}{i\alpha R}(D^2 - k^2)^2\phi = 0 \tag{40}$$

and

$$\hat{A}^{(n)} = \left[\int_0^{\infty} \tilde{\phi}^{(n)}(D^2 - k^2)\hat{v}_1\, dy\right] / I^{(n)}, \tag{41}$$

$$I^{(n)} = \int_0^{\infty} \tilde{\phi}^{(n)}(D^2 - k^2)\phi^{(n)}\, dy, \tag{42}$$

with $\tilde{\phi}^{(n)}$ being the eigensolutions of the adjoint problem. For the study of the long-time behavior, only the least damped mode need be considered. The Orr–Sommerfeld problem for the mean turbulent velocity profile was considered in Landahl (1967). To review the more important findings, we have replotted some of the numerical data obtained in that paper in a form suited to the present purpose. Figure 10 shows the real and imaginary parts of the least damped eigenvalue $c^{(0)} = c_r + ic_i$ for a range of wave numbers α and β. It is seen that the

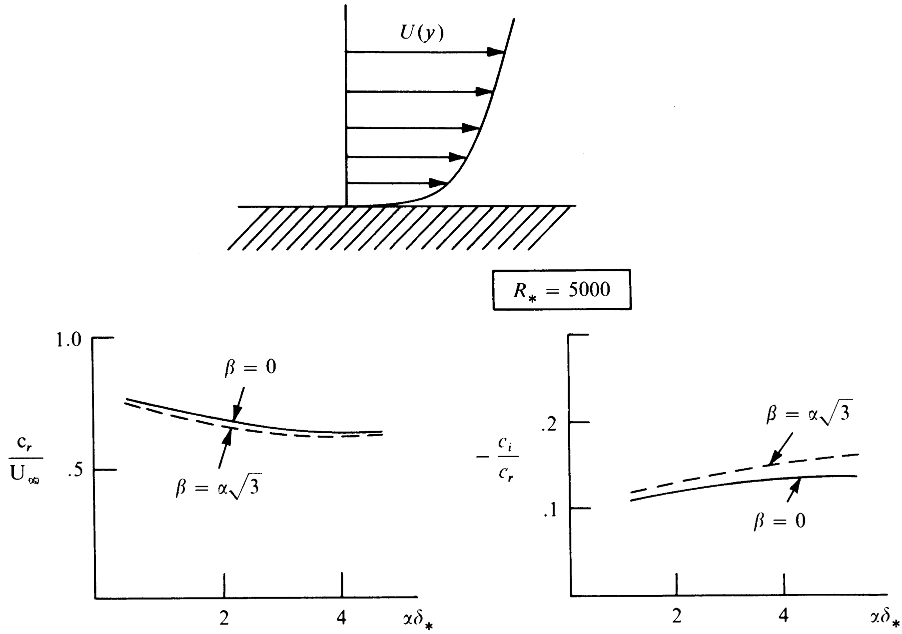

FIG. 10. *Wave propagation characteristics for the mean velocity profile (lowest mode)*

phase speed (the real part) decreases slowly with wave number from 0.8 of the free stream speed U_∞ at the low wave numbers to about $0.6U_\infty$ at the higher wave numbers. This behavior is as expected, since the higher wave numbers will involve motion closer to the wall where the mean velocity is lower. All waves are damped with a ratio of c_i/c_r only weakly dependent on α, showing that each wave component decays about equally much per cycle of oscillation. The decay rate obtained corresponds to a decay to an amplitude of $1/e$ within a distance of travel of approximately $1\frac{1}{2}$ wavelength. The mean flow is thus found to be quite stable, underlining the necessity for nonlinearities to maintain the fluctuating field. A very interesting property of the eigenvalues is also their very small dependence on β, which will be taken advantage of in trying to find an approximate inversion of the transform of (39). Since the eigenvalues and the eigenfunctions vary very little with β, one may, in carrying out the inversion integral over β, consider all factors to be independent of β, except the coefficient $\hat{A}^{(n)}$. Hence, including only the lowest mode one obtains from the inversion

$$(43) \qquad \tilde{v} \simeq \frac{1}{2\pi}\int_{-\infty}^{\infty} \exp\left(i\alpha(x - c_r t) + \alpha c_i t\right)\phi^{(0)}\bar{A}^{(0)}\, d\alpha,$$

where

$$(44) \qquad \bar{A}^{(0)} = \left[\int_0^\infty \tilde{\phi}^{(0)}\left(D^2 - \alpha^2 + \frac{\partial^2}{\partial z^2}\right)\bar{v}_1\, dy\right]\Big/ I^{(0)},$$

where $\bar{v}_1$ is the x-transform of $\tilde{v}_1$.

From this one can draw several interesting conclusions regarding the behavior of the $\tilde{v}$-field. First, it decays rapidly with the smallest wave number components having the largest life-time. With increasing time, the disturbances created by the burst will involve regions of flow at increasing distance from the wall, and the disturbances will propagate at an increased speed, i.e., the disturbance pattern will appear to lift up and accelerate downstream. In the limit of small α, we may approximate $\bar{v}_1$ by

$$\bar{v}_1 \simeq i\alpha \int_{-\infty}^{\infty} \tilde{f}_1 \, dx + \frac{\partial}{\partial z} \int_{-\infty}^{\infty} \tilde{f}_3 \, dx + \bar{v}_0, \tag{45}$$

and, upon neglecting α^2 and $\partial^2/\partial z^2$ compared to D^2 in consistency with earlier approximations made, we find

$$\bar{A}^{(0)} \simeq \frac{1}{I^{(0)}} \int_{-\infty}^{\infty} dx \int_0^{\infty} \tilde{\phi}^{(n)} D^2 [i\alpha \tilde{f}_1 + \tilde{f}_{3z} + \bar{v}_0 \, e^{i\alpha x}] \, dy. \tag{46}$$

What one sees from this result is that the spanwise structure will remain essentially unchanged during the decay of $\tilde{v}$, whereas the streamwise dimension will increase. Thus, an elongation of the disturbance $\tilde{v}$-field in the streamwise direction takes place during its decay.

The calculation of the $\tilde{u}$-field is somewhat more complicated. We will start from the first of (2) considering the nonlinear terms to be negligible in the time period after the completion of the burst. In order to be able to find a simple solution, we shall also assume the viscous terms to be negligible, an assumption that requires justification afterwards. Double Fourier transform of the equation for u under these assumptions then gives

$$\left(\frac{\partial}{\partial t} + i\alpha U\right)\hat{u} = -U'\hat{v} - \frac{i\alpha}{\rho}\hat{p}, \tag{47}$$

with initial condition

$$\hat{u}_{t=t_1} \equiv \hat{u}_1 \simeq -(D\tilde{f}_1)_{t=t_1}. \tag{48}$$

A suitable expression for the pressure is found by taking $\partial/\partial x$ of the first of (1) and adding it to $\partial/\partial z$ of the third component equation. After carrying out the Fourier transform, one finds (Landahl (1967, (18))) upon omitting nonlinear and viscous terms,

$$\hat{p} = -\frac{\rho}{k^2}\left[\left(\frac{\partial}{\partial t} + i\alpha U\right) D\hat{v} - i\alpha U'\hat{v}\right]. \tag{49}$$

One can now substitute this into (47), use the solution (39) for $\hat{v}$ as a function of time, and integrate the equation to find $\hat{u}$ subject to (48). This procedure yields

$$\begin{aligned} \hat{u} = {} & \left(\hat{u}_1 - \frac{i\alpha}{k^2} D\hat{v}_1\right) e^{-i\alpha U(t-t_1)} + \frac{i\alpha}{k^2} D\hat{v} \\ & - U'\left(1 - \frac{\alpha^2}{k^2}\right) \sum \frac{\hat{A}^{(n)} \phi^{(n)}(y)}{i\alpha(U - c^{(n)})} [e^{-i\alpha c^{(n)}(t-t_1)} - e^{-i\alpha U(t-t_1)}]. \end{aligned} \tag{50}$$

Of particular interest are the terms that will remain nonzero after an infinite time, viz.,

$$(51)\qquad \hat{u}_\infty = \left[\hat{u}_1 - \frac{i\alpha}{k^2}D\hat{v}_1 + U'\left(1 - \frac{\alpha^2}{k^2}\right)\sum \frac{\hat{A}^{(n)}\phi^{(n)}(y)}{i\alpha(U - c^{(n)})}\right] e^{-i\alpha U(t-t_1)}.$$

The inversion of this yields

$$(52)\quad \tilde{u}_\infty = \frac{1}{(2\pi)^2}\iint_{-\infty}^{\infty} e^{i(\alpha\xi+\beta z)}\,dk\left[U'\left(1 - \frac{\alpha^2}{k^2}\right)\sum \frac{\hat{A}^{(n)}\phi^{(n)}}{i\alpha(U - c^{(n)})} - \frac{i\alpha}{k^2}D\hat{v}_1\right] + \tilde{u}_1(\xi),$$

where $\xi = x - U(t - t_1)$. Since time enters only in this combination, (52) shows that the disturbance created by the burst will leave a "permanent scar" in the flow convected downstream with the local flow velocity. In reality, viscosity will of course make this disturbance decay, but on a time scale much greater than the decay time of the transient $\tilde{v}$-disturbances produced during the burst. The first term in (52) would be what would have resulted if the burst had only caused shear stresses without associated perturbations in $\tilde{v}$ and $\tilde{p}$. Then, in the absence of viscosity, each particle would have retained the velocity it had acquired during the burst. The second term of (52) contains both the effect of pressure gradients and the displacement of the fluid particles from their original y-position. The latter effect is most easily understood by considering the approximate equation for $\tilde{u}$ obtained by omitting both stress and pressure gradient terms, i.e.,

$$(53)\qquad \tilde{u}_t + U\tilde{u}_x \simeq -U'\tilde{v}.$$

The solution of this is easily found and can be demonstrated to be the linear counterpart of Prandtl's mixing-length hypothesis that each fluid particle would tend to retain its momentum as it is lifted through mixing to a different distance from the wall. The y-displacement, l, (the "mixing length") is given by, in linear approximation,

$$(54)\qquad l = \int_{t_1}^{t} \tilde{v}[x - U(t - \tau), \tau]\,d\tau,$$

where the integral is to be carried out at constant y and z. The solution for $\tilde{u}$ may then be written

$$(55)\qquad \tilde{u} = -U'l(\xi) + \tilde{u}_1(\xi).$$

On substituting the solution (39) into (54) and letting $t \to \infty$, one finds that the approximate solution (55) will reproduce the integral term of (52), except for the terms involving higher powers of α, which represent the effect of the pressure gradient. Such terms would be expected to be unimportant when the disturbance pattern becomes highly elongated in the streamwise direction. As was demonstrated above, the $\hat{v}$-field will elongate without substantial spanwise spreading during its decay, and a similar tendency, although perhaps not as strong, would be expected for the $\tilde{u}$-field. For a qualitative assessment of where large $\tilde{u}$-deficits may possibly arise so as to lead to a new breakdown condition, the approximate solution (54), (55) should be sufficient, however.

The integration path in the x, t-plane to be followed in (54) is shown in Fig. 11. The $\tilde{v}$-velocity field illustrated is what one would have in the case of an unswept

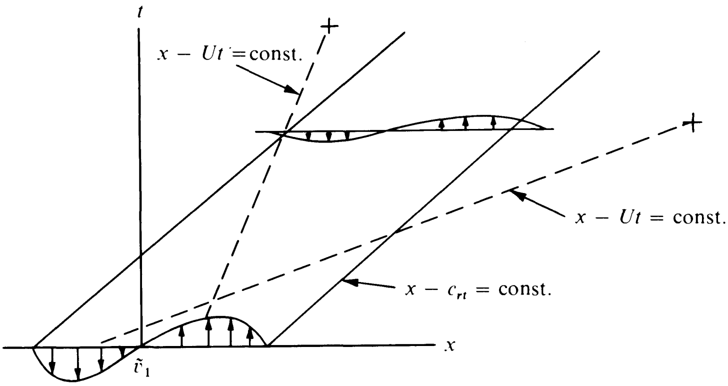

FIG. 11. *Integration path for evaluating mixing-length approximation*

breakdown with a zero spanwise stress component, as would be given at $t = t_1$ by (23) with $\tilde{f}_3 = 0$. This distribution pattern propagates along lines $x - c_r t \simeq$ const. and decays with increasing time. There is also some diffusive spreading because of $|c_i| \neq 0$. Two integration paths are considered, one for $U < c_r$ (the upper one) corresponding to small values of y and one for $U > c_r$, corresponding to larger values of y. The effect of the variation of c_r with wave number is ignored in this context, since this variation is so small that dispersion will have little time to spread out the wave pattern before the $\tilde{v}$-distribution has decayed.

Near the wall, the $\tilde{v}$-distribution will be negative (towards the wall) for small x and positive for large values with

$$\int_{-\infty}^{\infty} \tilde{v}\, dx = 0.$$

Therefore, for $U < c_r$, the net negative $\tilde{v}$-contributions to the integral will always be larger than or equal to in magnitude that from the region of positive $\tilde{v}$, so that l will be zero or negative, but never positive. A negative displacement of the fluid particles implies an increase in the $\tilde{u}$-perturbation, so that the net result will be a positive u-perturbation in the region close to the wall where $U < c_r$. For regions where $U > c_r$, the opposite will hold. The integration path will pass through regions of mostly positive $\tilde{v}$, so that a net positive l will result. Hence, for the unswept breakdown, the net change in $\tilde{u}$ will be in the same sense as that produced by the shear stresses during the burst.

For a swept breakdown, the induced $\tilde{v}$-values may be either positive or negative over the whole range of integration in x depending on whether the spanwise station studied lies to the left or the right of the center of the burst. Hence, the appearance of $\tilde{u}$-values of either sign will then be possible.

It is also of interest to consider the y-structure of the almost permanent $\tilde{u}$-perturbations created by the burst. First, it is important to notice from (51) that the perturbations may become particularly large near the "matched" layer, for which $U \simeq c_r$. The character of the perturbation will be different in the upper portions of the boundary layer for which U is mostly greater than c_r, than from what it is in the region closer to the wall, where the opposite is true. At larger values of y where $U > c_r$, the flow at a given station x will first feel—at a time $t \simeq x/U$, measured from the occurrence of the burst—the $\tilde{u}$-perturbations caused by waves having completed their y-displacement of the fluid particles at an early time, i.e., by the waves of the higher wave number regime. Because they have eigenfunctions with their maximum absolute values at smaller y-values than waves of lower α, the perturbation will be weak when the wave packet first arrives. The longer waves will arrive at a slightly later time because fluid particles will have time to move past the longer wave during its time of formation. As the effect of the smaller wave numbers are being felt, the disturbance will become stronger at increasing distances from the wall. To a stationary observer, the disturbance will therefore appear to travel away from the wall. For the region closer to the wall, for which U is less than c_r, the opposite picture will hold. The $\tilde{u}$-perturbation produced by the longer waves will arrive first, whereas those due to the shorter waves will arrive last. As the larger wave numbers are associated with disturbances having their maxima further out in the flow, the disturbance pattern, at a given x, will appear to move towards the wall.

5. A possible mechanism for burst regeneration. With the aid of the approximate solutions thus found for the disturbances created by a burst, we can make an assessment of whether sufficiently large $\hat{u}$-velocity defects could arise so as to lead to a new critical condition at some other point in the shear flow and thereby perpetuate the breakdown and the ensuing burst. First, we should recall that without the disturbances created by a burst, the flow would eventually decelerate near the wall to produce an inflexional region that would be unstable on the large scale. Thus, a new stress-producing inflexional-type instability must always eventually occur to maintain the turbulent velocity profile, whether of a localized or a large-scale nature. However, the slow-down of the velocity between bursts due to the viscous stresses acting on the mean velocity does not seem likely to be the main mechanism involved in the creation of a new instability. First, if this were so, the mean interval between bursts would scale with the wall parameters, but the experimental evidence tends to favor a scaling based on outer variables (Rao et al. (1971)). Second, there would be great difficulties with this mechanism to explain the occurrence of bursting in the outer, logarithmic layer, which has been observed in experiments (Kline et al. (1967)), although such bursts occur less often than in the wall region. Third, the observations of Kim et al. (1971) as well as by Blackwelder and Kaplan (1972) show the burst to be proceeded by a fairly rapid deceleration of the flow, according to Kim et al. (1971) being caused by the lift-up of a low-speed streak. Thus, an adequate model for burst regeneration would need to include the effect of the unsteady perturbations in setting up a new critical condition.

The results of the previous section also show that the displacement of fluid particles produced by the burst can cause semipermanent $\tilde{u}$-velocity perturbations that are particularly large near the matched layer where $U \simeq c_r$. In the viscous wall region, U is less than c_r for all but the highest wave numbers. An unswept burst was found to lead to a new displacement of fluid particles towards the wall and consequently would be expected to lead to a velocity excess in the wall region. Therefore, such a burst is not likely to produce a new critical condition in the inner wall region. A selective sampling technique such as the one employed by Blackwelder and Kaplan (1972) would give results typical of an unswept burst, since the sampling criterion does not distinguish between bursts of different orientation. Examination of their data show, indeed, that there is an acceleration of the fluid downstream of the burst (see last figure in Blackwelder and Kaplan (1972)).

We are therefore forced to conclude that with the present model, the regeneration of a new burst requires the appearance of sufficiently large spanwise stress components $\widetilde{v'w'}$, which could be produced in a swept burst. Such a component will induce an upflow in the spanwise section to one side of the burst and a downflow to the other side as described above. We are thus led to a tentative picture of the breakdown regeneration mechanism as illustrated in Fig. 12. The transient

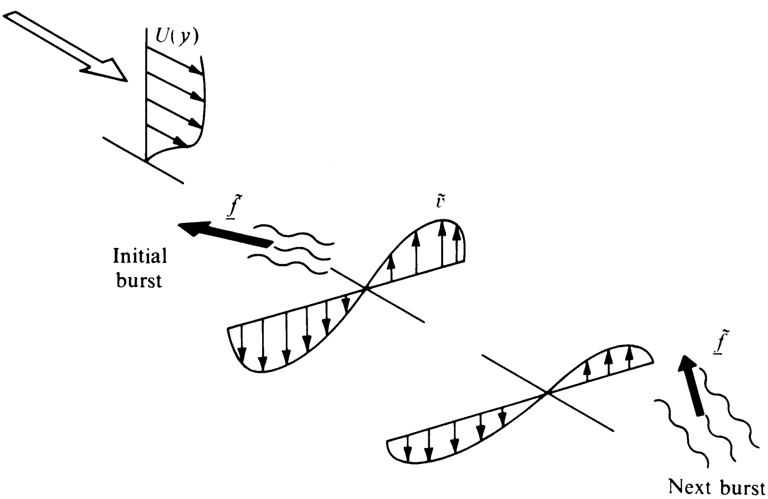

FIG. 12. *Possible burst regeneration mechanism* $(\overline{u'v'} = \iiiint \widetilde{u'v'}\, dV\, dt\,;\ \overline{v'w'} = \iiiint \widetilde{v'w'}\, dV\, dt)$

upflow generated to one spanwise side of the burst will have subsided after its decay time of typically $\tilde{\lambda}/|c_i|$, at which time the velocity defect has reached its maximum value. This may be strong enough to set off a new burst, which will appear downstream and slightly to the side of the original spanwise section. The upflow generated by the new burst may in turn give rise to a third one off to the side of the second one, and so on. Because of the alternating surface distribution pattern formed by subsequent bursts, the typical time before the appearance of a new burst in any particular spanwise section will be twice the decay time or more, giving a characteristic time between bursts at a given point of roughly

$$\overline{T}_B \simeq 2\frac{\tilde{\lambda}}{|c_i|}. \tag{56}$$

It should be noted that this result scales with outer-flow parameters. With

$c_i \simeq -0{\cdot}08\, U_\infty$ and a disturbance scale of typically δ_*, we find $\bar{T}_B \simeq 25\delta_*/U_\infty$. The good agreement with experiments such as those of Rao et al. (1971) which gave a mean time of $\bar{T}_B \simeq 30\delta_*/U_\infty$, is of course not too significant, since it depends on a fortuitous choice of scale such as whether or not a factor of 2π is included in the scale definition. What is relevant, however, is the finding that the time between burst is controlled by the large-scale motion with an evolution time set by outer-flow variables.

6. Conclusions. The model employed here presents the following qualitative picture of the fluctuating field in the wall region: the velocity field consists of a small-scale field coupled to a large-scale one through the strongly nonlinear mechanism of a burst. This is believed to be initiated when the large-scale velocity field becomes sufficiently inflexional to lead to a critical condition for breakdown in the sense of (I). The violent small-scale mixing produces large instantaneous turbulent stresses tending to smooth out the inflexional region and hence bring the profile back to a stable one. The large-scale motion induced thereby will, because of obliqueness of the bursting, be forcing fluid particles towards the wall to one side of the spanwise section and away from the wall on the other. Since the fluid particles will tend to retain the streamwise velocity they had at the start of the motion, a velocity defect will ensue in the spanwise region where an outflow is induced. This defect may lead to a new critical condition, and so on, so that a burst could perpetuate itself downstream without requiring the interaction with disturbances from other bursts.

A burst will leave behind "debris" of small scale u_i'-fluctuations, which will decay through viscous dissipation. The small-scale components are strongly correlated during the burst, producing typically high values of the shear stress components, $\widetilde{u'v'}$ and $\widetilde{v'w'}$, but the debris will be largely uncorrelated. The decay time of the large-scale $\tilde{v}$-fluctuations will be typical of the time required to produce a large velocity defect leading to a new burst, and gives therefore an estimate of the time interval between bursts that scales with outer-flow variables. In the inner wall region, there will also occur a slow deceleration of the mean flow between bursts as a result of the action of viscous mean stresses, which are unopposed by turbulent stresses during off-bursting periods.

The small-scale debris from the bursts and the large-scale $\tilde{u}$-fluctuations would not contribute significantly to the large-scale pressure fluctuations, which are associated with the $\tilde{v}$-component only, and therefore show a correlation typical of decaying waves. The success of the wave-guide model (Landahl (1967)) for describing pressure fluctuations could therefore not be expected to be duplicated for the velocity fluctuations, and efforts to fit the data on the latter into a statistical model by Lahey and Kline (1971) do indeed show the need to add a term representing "unorganized" motion to the one representing waves.

The large-scale $\tilde{u}$-perturbation created by the burst will eventually decay, but since this decay is due mainly to viscous diffusion and not to interaction with the mean shear, it will be much slower than that of the $\tilde{v}$-perturbation. Associated with the streamwise velocities, there must also appear a $\tilde{w}$-perturbation to satisfy continuity. The long-time, large-scale perturbation field will thus be essentially two-dimensional in each plane $y = \text{const.}$

The present model also allows us to make a tentative qualitative assessment of how the bursting will control the mean velocity distribution. The shear stress produced by a burst will add to the negative curvature of the mean profile. The increased curvature may lead to an enhanced stability to small disturbances, but more importantly, it will require a larger amplitude of the large-scale fluctuation before local inflexion, and hence secondary instability could set in. Thereby, the probability of the occurrence of a new burst will be decreased. Thus, the profile curvature is self-adjusting through the feedback of bursting to a value giving statistical equilibrium in the rate of occurrence of curvature-producing bursts. If the magnitude of profile curvature were to be increased through any outer means, for example, through a negative streamwise mean pressure gradient, the number of bursts required would go down and the profile would become more laminar-like. The decrease of bursting rate and the possibility of a complete relaminarization of a turbulent boundary layer in a strongly accelerating flow has indeed been demonstrated experimentally (Schraub and Kline (1965)).

There are several aspects of the model proposed which will need considerably deeper study to assess its validity and relevance. One of the most important ones is to determine whether the measured instantaneous velocity profile measured just prior to bursting is critical in the sense of the breakdown model. This requires numerical calculations of the local dispersion relation for the instantaneous profiles at and near this instant, which have not yet been completed. One possibly serious shortcoming in the basic model in light of the experimental evidence is the assumption of large streamwise and spanwise dimensions of the burst region in terms of the small-scale wavelength. Kim et al. (1971) found the spanwise extent of the burst to be only 10–30 in terms of the viscous wall length, which may be more typical of the small than of the large scale. A model allowing for a small spanwise scale may require inclusion of higher z-derivatives in the source term, as well as retainment of some of the other turbulent stress terms omitted in the present theory. Such a model would tend to accentuate the mechanism of formation of streamwise vortices and could possibly lead to an explanation of the counterrotating vortex pair structure of a spanwise scale of approximately $\lambda^+ = 100$ found to be present in the wall layer (Bakewell and Lumley (1967)).

A peculiarity of the model proposed is that for the large-scale field it will only allow for a "reverse" cascading, in that a burst occurring within a region of a scale $\tilde{\lambda}$ will produce motions of scale $\tilde{\lambda}$ or larger, but not of substantially smaller scale. Such a cascading process is completely at odds with the ideas of classical turbulence theory which assumes that the turbulent flow evolves continuously towards smaller and smaller scales until viscous dissipation provides a cut-off mechanism. For the turbulent boundary layer, such cascading would take place in the small-scale turbulence produced in the burst, but the main forward cascading would be a discontinuous one in wave number setting in when breakdown of the large-scale motion occurs.

REFERENCES

H. P. Bakewell and J. L. Lumley (1967), *Viscous sublayer and adjacent wall region in turbulent pipe flow*, Phys. Fluids, 10, 1880–1889.

R. Blackwelder and R. E. Kaplan (1972), *The intermittent structure of the wall region of a turbulent boundary layer*, Paper presented at 13th Internat. Congr. of Theoretical and Applied Mechanics, Moscow, August 1972. Also issued as Univ. S. Calif. Rep. USGAE 1–22.

E. R. Corino and R. S. Brodkey (1969), *A visual investigation of the wall region in turbulent flow*, J. Fluid Mech., 37, pp. 1–30.

W. Eckhaus (1965), *Studies in Nonlinear Theory*, Springer-Verlag, Berlin.

H. T. Kim, S. J. Kline and W. C. Reynolds (1971), *The production of turbulence near a smooth wall in a turbulent boundary layer*, J. Fluid Mech., 50, pp. 133–160.

S. J. Kline, W. C. Reynolds, F. A. Schraub and P. W. Runstadler (1967), *The structure of turbulent boundary layers*, Ibid., 30, pp. 741–773.

R. T. Lahey and S. J. Kline (1971), Rep. MD-26, Thermosciences Div., Dept. of Mech. Engrg., Stanford Univ., Stanford, Calif.

M. T. Landahl (1967), *A wave-guide model for turbulent shear flow*, Ibid., 29, pp. 441–459.

———, (1972a), *Drag reduction by polymer addition*, Applied Mechanics, Proc. 13th Internat. Congr. of Theoretical and Applied Mechanics, Moscow, August 1972, E. Becker and G. K. Mikhailov, eds., Springer-Verlag, Berlin, 1973, pp. 775–802.

——— (1972b), (I) *Wave mechanics of breakdown*, J. Fluid Mech., 56, pp. 775–802.

C. C. Lin (1955), *The Theory of Hydrodynamic Stability*, Cambridge University Press, London.

K. N. Rao, R. Narasimha and M. A. Badri Narayanan (1971), *The "bursting" phenomenon in a turbulent boundary layer*, J. Fluid Mech., 48, pp. 339–352.

F. A. Schraub and S. J. Kline (1965), *A study of the structure of the turbulent boundary layer with and without longitudinal pressure gradients*, Rep. MD-12, Thermosciences Div., Dept. of Mech. Engrg., Stanford Univ., Stanford, Calif.

J. M. Wallace, H. Eckelman and R. S. Brodkey (1972), *The wall region in turbulent shear flow*, J. Fluid Mech., 54, pp. 39–48.

W. W. Willmarth and S. S. Lu (1973), *Measurements of the structure of the Reynolds stress in a turbulent boundary layer*, Ibid., 60, pp. 481–511.